

Effect of nonlinear material behavior of laminated composite plates with central rectangular hole subjected to out -of- plane loading

*Ghazi Abu-Farsakh¹, * Yasser Hunaiti², and Asaad Al Bustami²*

¹Jordan University of Science and Technology, Civil Engineering Department, Irbid, Jordan

²Jordan University, Civil Engineering Department, Amman, Jordan

Abstract. The purpose of this paper is to investigate the effect of nonlinear material behavior on four layered, symmetric; angle-ply laminated composite plate with various fiber-orientation angles; ($\theta = 30^\circ, 45^\circ$ and 60°). The plate has a central square-hole and subjected to out-of-plane uniformly distributed load. The effect of Stress Concentration Factor (SCF) resulting from redistribution of in-plane stresses ($\sigma_x, \sigma_y, \tau_{xy}$) around the hole was taken into consideration. Square plates with simply supported boundary conditions were considered in the present study. The analysis was carried out utilizing the ANSYS-computer program. The presence of a central hole was found to concentrate the maximum stresses at the corners of the hole. The nonlinear material behavior was found to redistribute the in-plane stresses more reasonably and smoothly around the hole-perimeter and hence resulting in smaller SCF-values.

1 Introduction

In engineering science, composite materials can be generally defined as any material that has been physically assembled from two or more materials to form one single bulk material with new properties. The resulting composite material will have the advantages of good characteristics of each constituent material.

A common type of composite materials is known as the fibrous composites; which mainly consist of two separate components; the matrix and the fibers. The matrix component will act as the adhesive material that holds the fibers together to form the bulk of the composite material. It usually consists of various types such as: epoxy, polymer, metal and thermoplastic. The fibers are of different types such as: Carbon, Boron, Graphite and Kevlar. The matrix and fibers together form what is known a lamina. Combination of several laminas form what is known as a laminated composite. Lamination is used to

* Corresponding author: ghazi@just.edu.jo

combine the best aspects of the constituent layers in order to achieve a more useful material. The properties that can be emphasized by lamination are strength, stiffness, low weight, corrosion resistance, etc., as indicated in [1]. Jones, 1975.

It is well known that a rectangular plate with a rectangular hole has been widely used in industrial designs such as: Civil, Mechanical, Marine and Aeronautical Engineering. Composite materials as: Graphite/Epoxy, Boron/Epoxy, and Glass/Epoxy are widely used in structural components in military (Stealth fighter F-117A Nighthawk and B-2 bomber) and commercially (for example: the forthcoming Boeing 787 Dreamliner airplanes), because of the advantage of weight saving, hence, achieving high strength-to-weight ratios in various components. Furthermore, providing enhanced corrosion resistance and improved stealth characteristics. Best composite design was achieved through the variation of stacking pattern and fiber-orientation.

Linear and nonlinear structural behavior of composite plates and shells was investigated by several researchers using the finite element method with a variety of approaches. Most of the researches were concerned with the problem of geometric nonlinearity of large or moderately large deformations. Han et al. [2] used the hierarchical finite element method to carry out the geometrically nonlinear analysis of laminated composite rectangular plates, utilizing the first order shear deformation theory and Timoshenko's laminated composite beam functions. Zinno et al. [3] used the Lagrange approach to develop a three-dimensional element with two-dimensional kinematic constraints for the geometric nonlinear analysis of laminated composite plates.

Ganapathi et al. [4] presented an eight-node quadrilateral finite element based on the Reissner-Mindlin plate theory to analyze thick laminated composite plates accounting for moderately large deformations. Polit et al. [5] studied the geometrically nonlinear behavior using a high order triangular finite element plate model having six nodes. The element ensured continuity of transverse interfacial shear stresses of multi-layered composite plates.

Zhang et al. [6-8] developed a four-node quadrilateral elements for linear and geometrically nonlinear analysis of thin to moderately thick laminated composite plates. Khoa et al. [9] developed a rectangular non-conforming element based on Reddy's higher order shear-deformation plate theory to analyze the laminated composite plates. Further studies were carried out on the subject of geometric nonlinearities by other investigators; Salehi et al. [10], Choudhary et al. [11] and many others.

Several researches were carried out on the effect of fiber-orientation, number of plies and laminate-sequence in reducing weight of symmetric and anti-symmetric laminated composite plates subjected to uniform pressure loads; Naghipour et al. [12] developed an analytical procedure to investigate the bending-stretching significance of anti-symmetric and cross-ply laminated composite plates based on a higher order shear displacement model using zigzag-function.

A limited research was carried out on the problem of material nonlinearity and its effect on the behavior of composite laminated plates, especially, in the case of a plate with holes. Abu-Farsakh et al. [13] studied the problem of stress-concentration around a central circular hole in fibrous composite laminated plates subject to in-plane tensile loading. The main aim of the research was to investigate the effect of material nonlinearity on stress-concentration and stress-redistribution around the hole.

For studying the behavior of composite materials with holes, the ANSYS-computer program [14] will be used to account for the stress-concentration and resulting stress-redistribution caused by the presence of holes. Stress-concentration is an important parameter to be taken into consideration in structural design, because the point near maximum stress-concentration zone is often the location of damage initiation in the structure

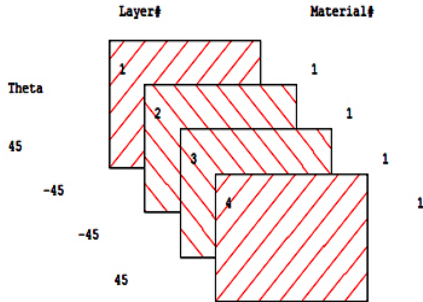
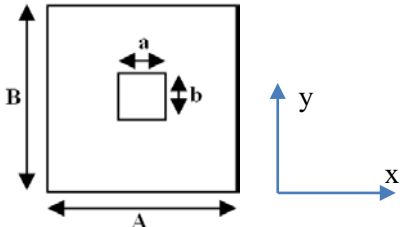
2 Scope and objectives

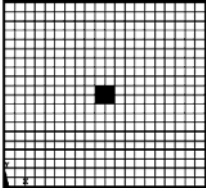
The main objective of the present paper is to investigate the effect of linear and nonlinear material behavior on the induced in-plane stresses (σ_x , σ_y and τ_{xy}) in simply supported square plates and then to obtain the corresponding Stress-Concentration Factors (SCF). Plates have symmetrical angle-ply laminates composed of four layers $[\Theta/-\Theta]_s$. The effect of fiber-orientation angle (Θ) is taken into consideration using three values; 30, 45 and 60-degrees. All plates are subject to out-of-plane uniformly distributed loads of intensities 2.5 MPa and 5 MPa.

3 Application of ANSYS finite element model

The ANSYS-computer program is used for both linear and nonlinear analysis. In linear analysis; element-type SHELL99 is used while for nonlinear analysis element-type is SHELL91. Each of the elements have eight nodes with six degrees-of-freedom at each node; three translations and three rotations. A summary description of element-type, element-geometry, composite-material, number of plies, fiber-orientation angles, plate dimensions and boundary conditions are as indicated in Table (1).

Table 1. Summary description of ANSYS applications.

Title	Description
<p>Number of Layers</p>	<p>Four layers, with ply thickness 2.5 mm each. The fiber-orientation angles are 30°, 45° and 60° having staking-sequences in the laminate as $[+\theta^{\circ}/-\theta^{\circ}]_s$. Angle ($\theta$) is taken with respect to the positive x-axis, where x and y are body global axes.</p> 
<p>Plate Geometry</p>	 <p>$A=B= 100 \text{ mm}$ $a=b= 10 \text{ mm}$</p>

<p>Mesh Generation</p>	<p>Due to using shell element, the mapped mesh on the area is created as indicated in the figure, and then the number of divisions required for mapped mesh is specified.</p> 	
<p>Boundary Conditions</p>	<p>All edges simply supported: $U_x = U_y = U_z = 0$, $\Theta_x \neq 0$, $\Theta_y \neq 0$, $\Theta_z \neq 0$</p>	<p>The simply supported conditions for all edges are used.</p>
<p>Loads</p>	<p>An out-of-plane uniformly distributed load of intensity 5 MPa.</p>	<p>An out-of-plane uniformly distributed load of intensities 2.5 and 5MPa.</p>

4 Nonlinear material model

The nonlinear mechanical properties of the composite material are expressed as [15-17]:

$$M_i = M_o \left[1 - B_i (\bar{U}_p)^{C_i} + D_i (\bar{U}_p) \right] \tag{1}$$

Where,

M_i, M_o : Secant and tangential mechanical properties

B_i, C_i, D_i : Material-property constants for mechanical property (i).

Three in-plane mechanical properties; E_1, E_2 and G_{12} , are expressed using Eq. 2. The initial values of mechanical properties and the corresponding material constants are as indicated in Tables 1 to 2. The plastic strain energy term (\bar{U}_p) is normalized as:

$$(\bar{U}_p) = \frac{U_p}{U_o} = \frac{U_s - U_e}{U_o} \tag{2}$$

For in-plane stress case, the total secant strain energy density (U_s) may be expressed in terms of principal material directions (1 & 2) as:

$$U_s = \frac{1}{2} \left(\frac{\sigma_1^2}{E_1} + \frac{\sigma_2^2}{E_2} + \frac{\tau_{12}^2}{G_{12}} \right) \tag{3}$$

Where, E_1, E_2 and G_{12} are the secant moduli at each stress level.

Similarly, the initial elastic moduli E_{o1}, E_{o2} and G_{o12} can be used to obtain the elastic strain energy density, such that:

$$U_e = \frac{1}{2} \left(\frac{\sigma_1^2}{E_{o1}} + \frac{\sigma_2^2}{E_{o2}} + \frac{\tau_{12}^2}{G_{o12}} \right) \tag{4}$$

The plastic strain energy density (U_p) is obtained (as shown in Fig. 1) as:

$$U_p = U_s - U_e \quad (5)$$

The term (U_o) is used to normalize the plastic strain energy density, and it is usually taken equal to unity (i.e. 1 MPa).

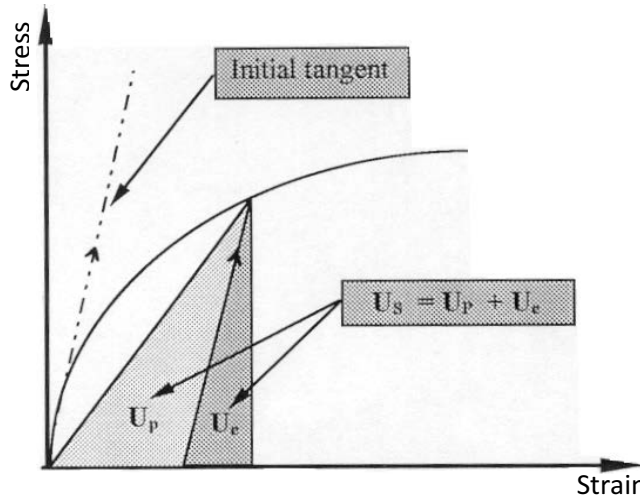


Fig. 1. Typical non-linear stress-strain curve for the *ith*-mechanical property showing the strain energy density terms.

The normal-stress versus normal-strain relation ($\sigma_x - \varepsilon_x$), see Table-1 for x-axis, was predicted using the nonlinear material model which was originally developed by the first author [15]. In order to account for the nonlinear material behavior, a computer program MCOMP was developed for this purpose. Every layer in the composite laminate was defined as a new material-type having a specific orientation-angle (Θ). Accordingly, the material model was properly incorporated in the ANSYS-computer program in the material-property section. The stress-strain relationship was dealt with as a multi-linear fitting technique for the provided stress-strain graph. The computer program utilized the **Newton-Raphson** technique to achieve step-convergence at each increment.

5 Analysis of results and discussion

The stress-distribution profile was greatly affected due to the existence of a central square hole. Thus, allowing for the redistribution of stresses around the hole to take place. Hence, allowing the stresses to change sign from tension to compression in the vicinity of hole-corners with increased maximum stresses in the nearby region. In this paper the simply supported boundary conditions will be considered only, as indicated earlier in Table 1.

The stress-distribution profiles (σ_x , σ_y , and τ_{xy}) due to uniformly distributed load intensity of 5 MPa for the case of simply supported square plate ($A/B=1$) and a square hole ($a/b=1$), versus x-distance are illustrated in Figures 2-a, 2-b and 2-c, respectively. For the case of $\Theta=30^\circ$. In the linear analysis case, the stress-distribution (σ_x) showed a maximum

value for $\Theta=30^\circ$ (about 205 MPa at $x=35$ mm). On the other hand, the maximum compressive stresses reached 135.38 MPa, on the hole-perimeter ($x=45$ mm) due to the redistribution of stresses process. With respect to the nonlinear analysis, the maximum tensile stress (σ_x) reached 174.22 MPa at $x=25$ mm, while the maximum compressive stress was 9.887 MPa at $x=45$ mm.

In the present paper, the Stress Concentration Factor (SCF) is defined as:

$$\text{SCF} = \frac{\text{Maximum stress with hole}}{\text{Maximum stress without hole}} \quad (6)$$

This factor is affected by hole-size (a/b), plate-size (A/B), fiber-orientation angle (θ), and boundary conditions of the plate.

The Stress-Concentration-Factor (SCF) as affected by the fiber-orientation angle due to in-plane stresses (σ_x , σ_y and τ_{xy}) for the case $A/B=1$ with a central square hole ($a/b=1.0$), is illustrated in Figure 3. Three fiber-orientation angles are taken in to consideration; 30, 45 and 60-degrees. A well-known composite material is considered herein in order to compare linear with nonlinear behaviors using Narmco-5605 Graphite/Epoxy composite material. The nonlinear in-plane shear properties according to Eq. (1) are given as: $B_{12}=0.562625$, $C_{12}=0.395999$ and $D_{12}=0.112317$. Material properties in 1 and 2 principal material directions are considered linear with initial moduli $E_{10}=1.062 \times 10^4$ MPa, $E_{20}=1.276 \times 10^5$ MPa and $G_{120}=5.861 \times 10^3$ MPa.

With respect to SCF, obtained linear values ranged approximately between (2.2 to 2.4), while the corresponding nonlinear values ranged approximately between (1.1 to 1.5) at all Θ -values for all stresses, as shown in Figures 3-a, 3-b and 3-c. As indicated, the maximum stress-values obtained from nonlinear analysis at the hole-sides are decreased and stresses are subjected to redistributions around the hole-perimeter and become smoother (i.e. no sharp peaks). Hence, the resulting SCF obtained from nonlinear analysis are smaller than those obtained from linear analysis.

Other comparisons using the nonlinear analyses under out-of-plane uniformly distributed loads of 5 and 2.5 MPa intensities are shown in Figures 4-a, 4-b and 4-c. The stress distributions (σ_x , σ_y and τ_{xy}) are exhibited for the plate case ($A/B=1$), hole-ratio ($a/b=1$) and $\Theta = 30$ -degrees. As the load is increased from 2.5MPa to 5 MPa, maximum σ_x -stresses are increased accordingly in a variable manner. That is, at the load 5 MPa the rate of increase was higher at $\Theta = 30$ -degrees and decreased gradually at bigger angles ($\Theta = 45$ and 60-degrees); see Figure 4-a. On the other hand, the maximum σ_y -stresses are increased gradually with increased fiber-orientation angle (Θ), as illustrated in Figure 4-b. In-plane shear stresses (τ_{xy}) showed almost a linear decreasing-rate with increased fiber-orientation angles but with steeper slope for the 5 MPa load-intensity compared to the 2.5 MPa intensity, as indicated in Figure 4-c.

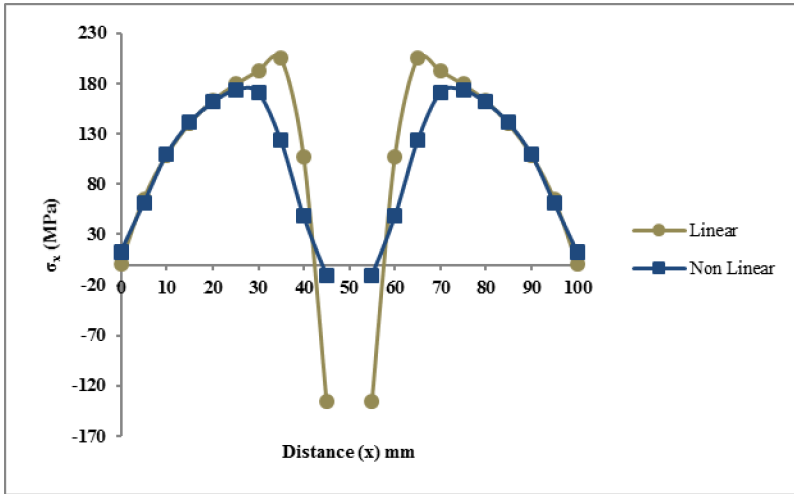


Fig. 2-a. In-plane stress-distribution (σ_x) versus distance (x); $A/B=1$, $a/b=1$ and $\Theta = 30^\circ$.

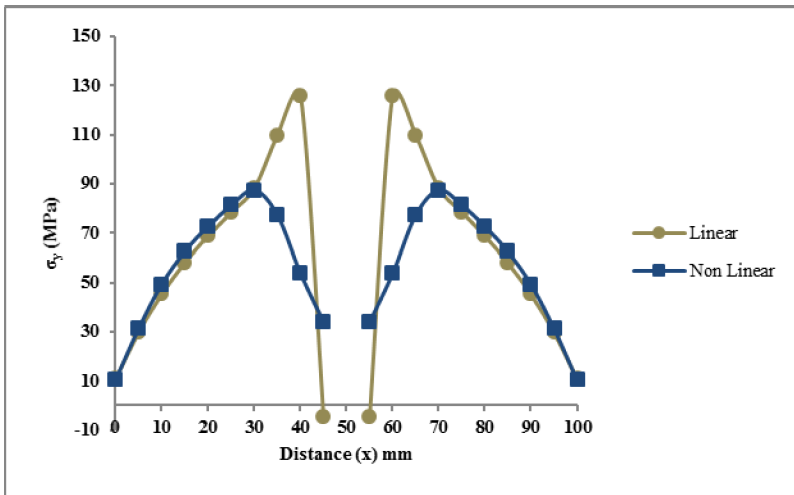


Fig. 2-b. In-plane stress-distribution (σ_y) versus distance (x); $A/B=1$, $a/b=1$ and $\Theta = 30^\circ$.

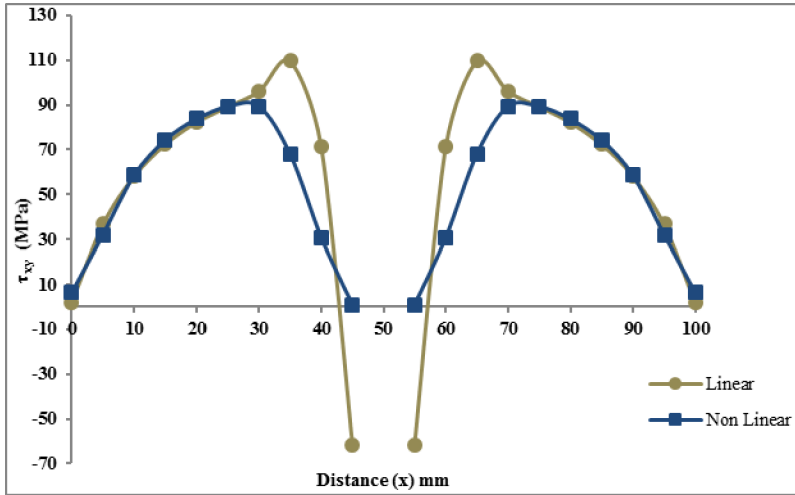


Fig. 2-c. In-plane stress-distribution (τ_{xy}) versus distance (x); $A/B=1$, $a/b=1$ and $\Theta = 30^\circ$.

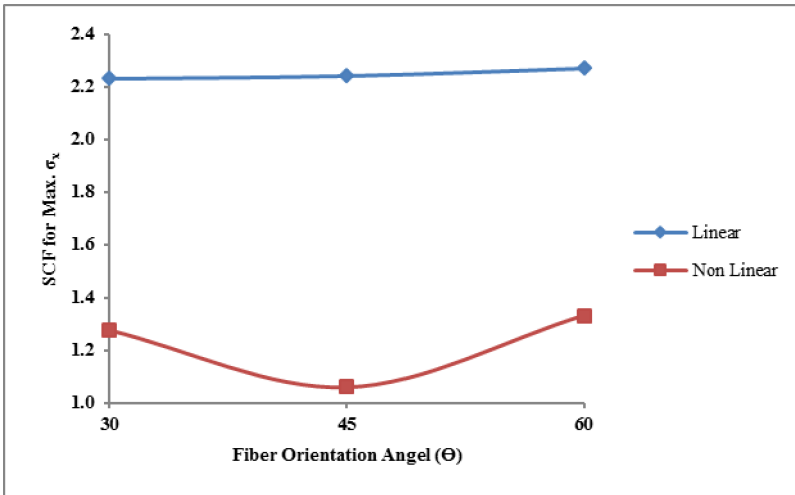


Fig. 3-a. SCF for maximum (σ_x) versus Θ ; $A/B=1$, $a/b=1$ for the uniformly distributed load of 5 MPa.

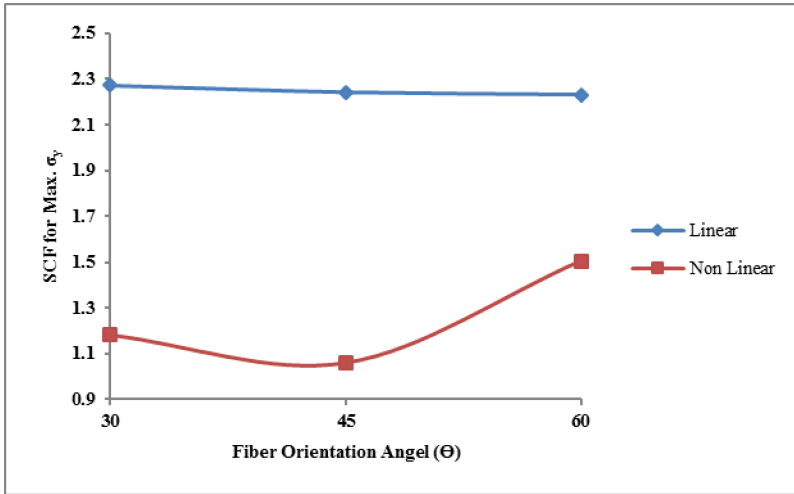


Figure 3-b. SCF for maximum (σ_y) versus Θ ; $A/B=1$, $a/b=1$ for the uniformly distributed load of 5 MPa.

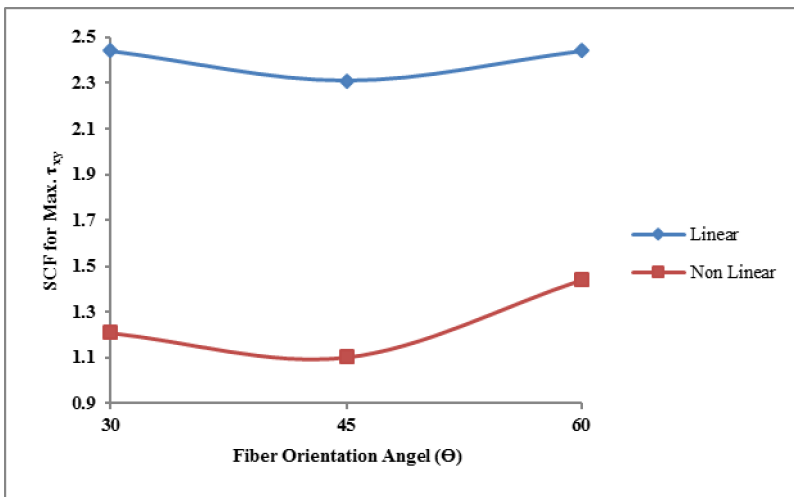


Figure 3-c. SCF for maximum (τ_{xy}) versus Θ ; $A/B=1$, $a/b=1$ for the uniformly distributed load of 5 MPa.

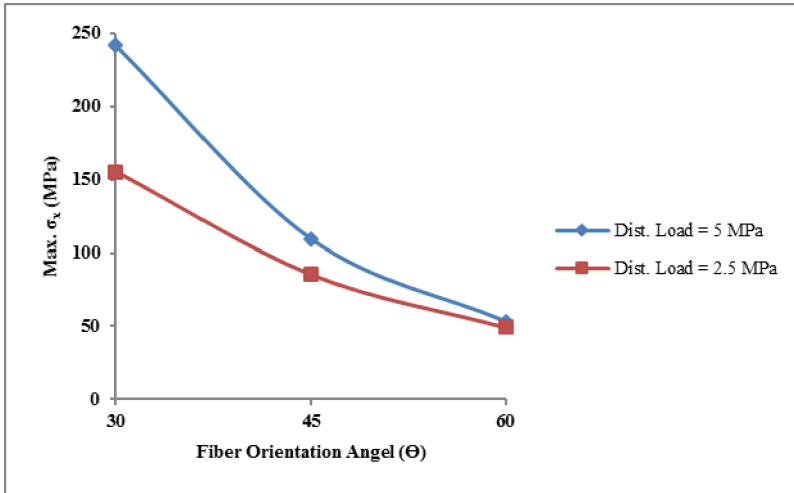


Figure 4-a. Maximum (σ_x) versus Θ ; $A/B=1$, $a/b=1$ for the uniformly distributed loads of 5 and 2.5 MPa.

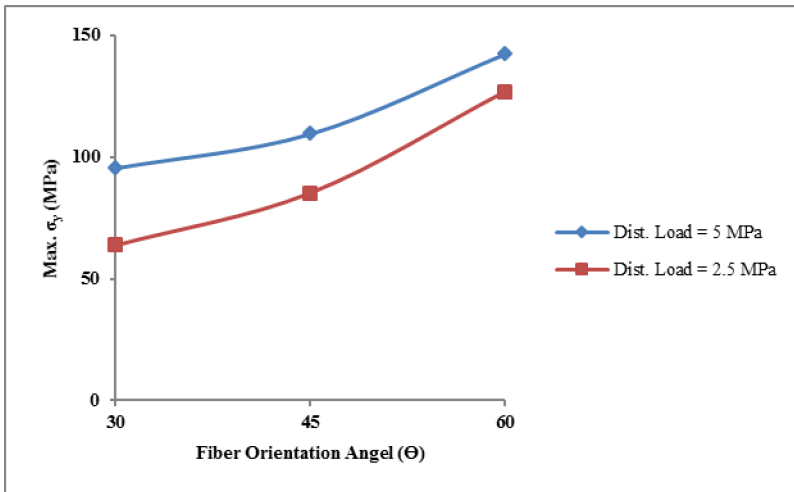


Fig. 4-b. Maximum (σ_y) versus Θ ; $A/B=1$, $a/b=1$ for the uniformly distributed loads of 5 and 2.5 MPa.

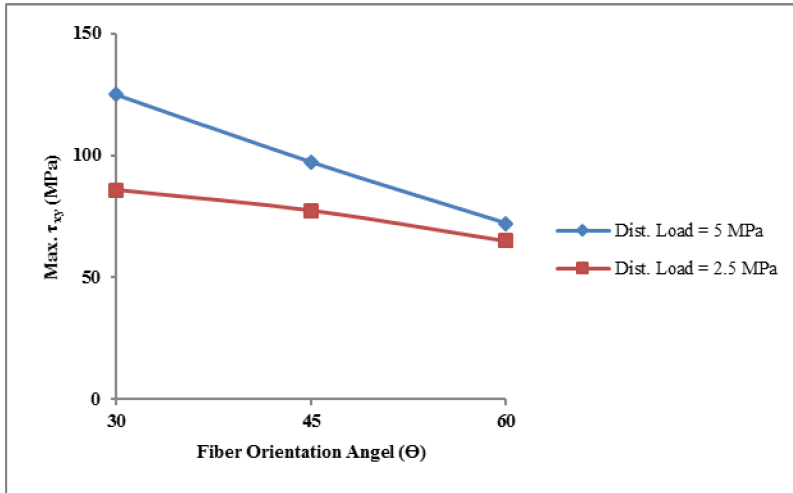


Fig. 4-c. Maximum (τ_{xy}) versus Θ ; $A/B=1$, $a/b=1$ for the uniformly distributed loads of 5 and 2.5 MPa.

As illustrated in Figure 5, stress values are decreased as we move away from the hole, and the nodal results in the nonlinear analysis showed discontinuity at corner nodes of the hole. Thus, the allowable stresses will be exceeded in the hole-vicinity.

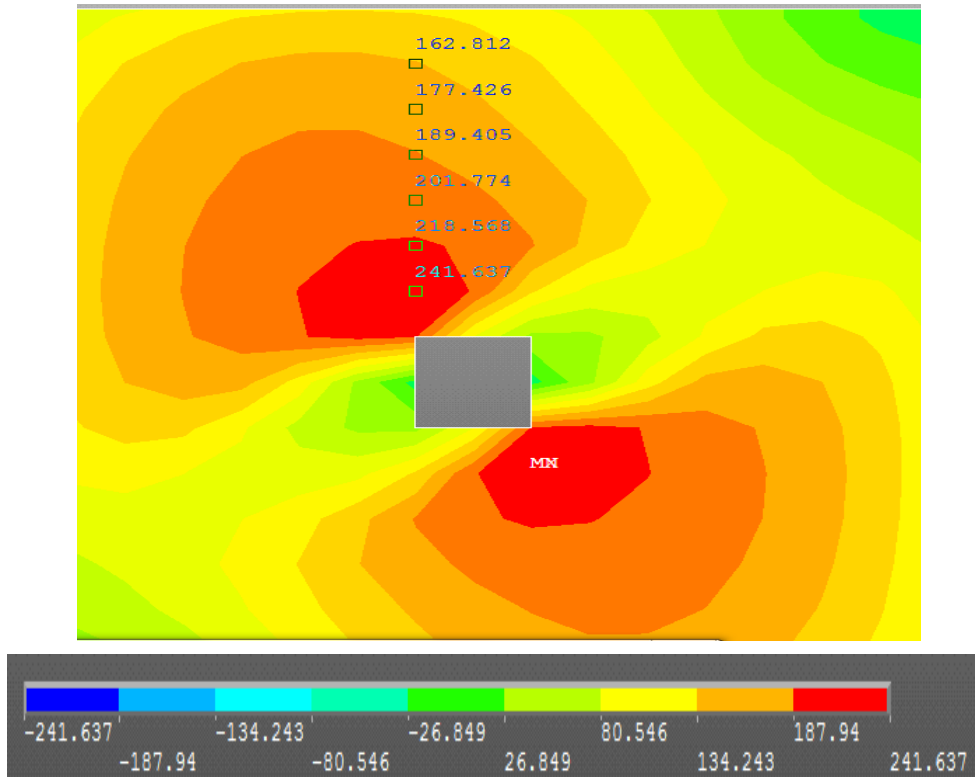


Fig. 5. A representative figure showing stress- σ_x contours for the square plate with a square hole for the case $\Theta = 30^\circ$.

6 Conclusion

Several parameters showed an increasing effect on the stress-concentration phenomenon in rectangular plates with central square hole and subjected to uniformly distributed loading, such as: plate aspect-ratio, hole aspect-ratio, fiber-orientation angle, plate boundary conditions and method of analysis; linear or nonlinear. In the present paper two factors were discussed; fiber-orientation angle and method of analysis due to space limitations.

Maximum stresses around the hole-perimeter resulted from linear analysis showed larger values than those corresponding to nonlinear analysis. This was attributed to the stress-redistribution process which occurred in the vicinity of the hole due to the nonlinear material behavior.

For the considered fiber-orientation angles (30, 45 and 60-degrees), the range of Stress Concentration Factors (SCF) using linear analysis was approximately in the range of (2.2 to 2.4), while the corresponding range for nonlinear analysis was approximately (1.1 to 1.5).

References

1. R. M. Jones. *Mechanics of Composite Materials*. New York: McGraw-Hill (2011)
2. W. Han., K. M. Petyt, F. E. Anal. Des. **18**(1–3), pp. 273–288 (1994)
3. R. Zinno, E. J. Barbero, *Comp. Struc.*, **57**(3), pp. 455–466 (1995)
4. M. Ganapathi, O. Polit, M. Touratier. *Int. J. Num. Meth. Eng.*, **39**(20), pp. 3453–3474 (1996)
5. O. Polit, M. Touratier, *Compos. Struc.*, **58** (1), pp. 121–128 (2002)
6. Y. X. Zhang, K. S. Kim, *Int. J. Num. Meth. Eng.*, **61**, pp. 1771–1796 (2004)
7. Y. X. Zhang, K. S. Kim, *Comp. Meth. Appl. Mech. Eng.*, **194**, pp. 4607–4632 (2005)
8. Y. X. Zhang, K. S. Kim, *Compos. Struc.* **3**, pp. 301–310 (2006)
9. N. N. Khoa, T. I. Thinh, *Viet. J. Mech.*, VAST, **29** (1), pp. 47–57 (2007)
10. M. Salehi, S. R. Falahatgar, *Trans. B: Mech. Eng.* **17** (3), pp. 205-216 (2010)
11. S. S. Choudhary, V. B. Tungikar, *Int. J. Eng. Sci. Tech.*, **3** (6), pp. 4897-4907 (2011)
12. M. Naghipour, H. M. Daniali, K. S. H. A. Hashemi, *W. App. Sci. J.*, **4** (5), pp. 681-690 (2008)
13. G. Abu-Farsakh, A. Almasri, D. Qa'dan, *Sci. Eng. Compos. Mat. (SECM)*, **22** (1), pp. 31-36 (2015)
14. *ANSYS Tutorial*, Release 9.0.
15. G. A. Abu-Farsakh, *Compos. Sci. Tech.*, **20** (4), pp. 349–360 (1989)
16. G. A. Abu-Farsakh, Y. A. Abdel-Jawad, *J. Compos. Tech. Res.*, (JCTRER), **16** (2), pp. 138-145 (1994)
17. G. A. Abu-Farsakh, Y. A. Abdel-Jawad, *J. Compos. Tech. Res.* (JCTRER), **17** (2), pp. 90-98 (1995).